Journal of Hazardous Materials, 7 (1983) 223–232
Elsevier Scientific Publishing Company, Amsterdam — Printed in The Netherlands

THE FLOWING AFTERGLOW IN ARGON AND HELIUM: DIFFERENCES IN TWO REACTOR DESIGNS IN APPLICATION TO THE ANALYSIS OF MOISTURE.*

R. I. BYSTROFF and N. D. STOUT
Lawrence Livermore National Laboratory, Livermore, California

ABSTRACT

Excitation by rare gas metastables in a glow discharge afterglow is effective for the sensitive chemiluminescent detection of trace moisture. In the development of a flowing afterglow (FLAG) system for the study of effluent gases from high explosives, two approaches were taken in the design of a modular reactor. A glass reactor system with a tantalum shell hollow cathode source isolated by a Woods horn was compared to a 3 in. dia. steel reactor in which the reactor entrance port acts as the cathode. The sensitivity of both systems increases linearly with currents up to 15 mA in operation at 1 Torr argon or helium. The steel reactor provides an order of magnitude greater sensitivity for OH than the glass reactor. A continuous moisture background at 60°C over vacuum dried nitrocellulose of 0.9 nmol/gm-s (0.02 ppm) is demonstrated. With the steel system a photon count sensitivity for OH at 308.9 nm of 30000 counts/nmol in argon and 5200 counts/nmol in helium is obtained using a 0.4 nm bandpass.

INTRODUCTION

The long-term stability of organic materials is often inferred from the rate of production of various gaseous products. However, elevated temperatures are frequently necessary to obtain requisite quantities for measurement, and decomposition rates cannot reliably be extrapolated to obtain the rates at near-room temperature. Moreover, as the temperature approaches ambient conditions, the interpretation of batch outgassing is made more difficult because of the competing significance of solubility, permeation, diffusion and desorption processes, and side reactions. In addition, the long storage times and limited collected sample tax the analytical measurement. The problem is alleviated somewhat by analytical speciation, provided the decomposition is

*Work performed under the auspices of the U. S. Department of Energy at the Lawrence Livermore National Laboratory under contract W-7405-Eng-48.

characterized by unique molecular products. The flowing afterglow (FLAG) technique provides for the very sensitive chemiluminescent detection of specific molecular species of interest in decomposition and compatibility studies.

In the FLAG technique, a glow discharge in an inert gas such as argon or helium acts as a source of highly energetic metastable atoms. The gas surrounding the glow is caused to flow with a linear velocity exceeding the radial diffusion of atoms to the walls, where energy loss can occur. Because the metastable lifetimes greatly exceed those of other excited species created in the glow, at some point downstream of the glow, the gas consists primarily of neutral and metastable inert gas atoms. It is at this point that a secondary gas stream, that has passed through a sample pyrolysis chamber is mixed with the source stream, and metastable-induced chemiluminescence is produced. Efficient transfer of energy to a sample molecule depends on an energy match between the excitant atom and some vibronic excited state in the sample molecule. Ionization or dissociation may also occur. The metastable excitation, therefore, tends to be highly specific compared to purely electronic excitation, and the chemiluminescent spectra often consists of simple progressions of relatively narrow vibrational bands, characteristic of di- and triatomic molecules and ions. These bands are resolved with low-resolution, high speed optical monachromators. Table 1 lists some of the species easily detected with argon and helium FLAG metastable transfer excitation spectroscopy (acronym: MTES) with high sensitivity.

Table 1. Species detected in Ar and He afterflows with high sensitivity. Only species easily identified with the low resolution systems described are included.

Argon	Helium
N_2 $C_3\Pi_u$	N_2^+ $B^2\Sigma_u^+$
OH $A^2\Sigma^+$	OH $A^2\Sigma^+$
CN $B_2\Sigma^+$	CO^+ $B^2\Sigma$
CH $A^2\Delta$	CO_2^+ $A^2\Sigma^+$
NH $A^3\Pi$	H(I)

The FLAG system used in this study resembles the glass system described by others (refs. 1-3). However, in order to test the feasibility of a modular system, the system was first constructed of steel. Subsequently, a glass reactor module was substituted for the steel reactor, and the qualitative

differences are described here, particularly in application to the analysis of moisture.

EXPERIMENTAL

The system, showing the glass reactor in place, is shown schematically in Fig. 1. The cylindrical steel reactor module is shown in Fig. 2.

Carrier Gases

Helium and argon were obtained prepurified to 99.9995 percent. The titanium trap efficiency for scavenging nitrogen was measured by following the 391 nm N_2^+ band intensity in a helium discharge as the trap temperature was raised. No further improvement occurred above 550°C. To remove residual water, a liquid nitrogen coil trap was installed on the low pressure side of the plasma throttling valve to limit argon condensation. The coil length of 1 m was necessary because of the high linear flow rates employed.

Calibration

Calibration for moisture determinations were performed by injecting a 50 µL to 3 mL sample of water-saturated He or Ar through a septum adapted to the pyrolysis tube flange. Selected gas-tight plastic syringes with 26 gauge hypodermic needles, calibrated for volume, were found suitable. The interior of the pyrolysis tube was coated with a thin film of teflon, which demonstrably reduced tailing of OH signals. The exponential decay of signal was integrated with a digital integrator (ECO Mod. 731), and the trace recorded. The carrier flow was typically held to less than 1 percent of the plasma gas flow. Nitrogen and other permanent gases, diluted 1:100 in the carrier gas, were added through the calibrated vernier inlet valve to provide steady state calibration signals. The operating conditions are summarized in Table 2.

RESULTS

The Steel Reactor

The luminescence in the steel reactor was first studied as a function of pressure, current and, in a coarse way, distance from the plasma inlet. The current could be increased to 200 mA, but in excess of ca. 15 mA, the complexity of the spectra increased. Argon lines and continua increased, and at high currents the nitrogen 1st positive spectra appeared, suggesting that recombination processes and electronic excitation predominate. However, with currents up to 15 mA, the spectra in argon was simply that of OH ($A^2\Sigma^+ - X^2\Pi$) and the second positive vibrational system of nitrogen ($C^3\Pi_u - B^3\Pi_3$), from residual

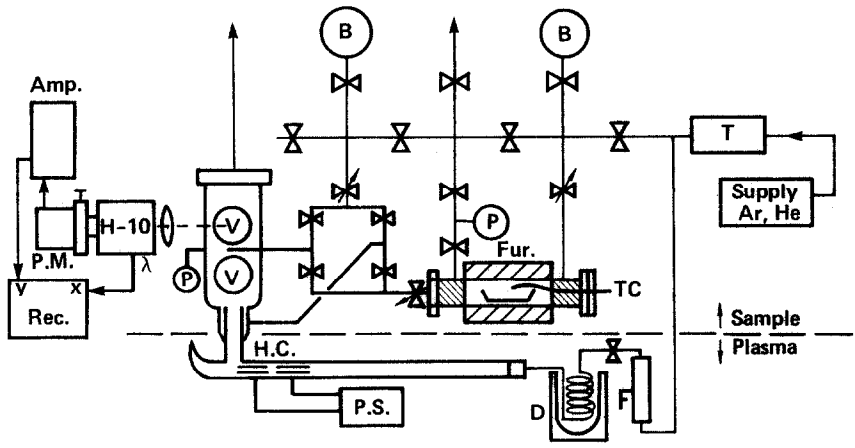

Fig. 1. System schematic and detail: right to left, regulated argon and helium is further purified by a 600°C titanium trap, T. Plasma section: The major flow, 25 scc s^{-1}, passes through flowmeter, F, a throttling valve, and the remaining H_2O is trapped in LN with a 1 m, 6 mm dia. coil at reduced pressure before passing through a 35 cm long plasma tube, equipped with two 2 x 1 cm cylindrical tantalum shells and a Woods horn. The glow discharge is sustained by a 200 VDC power supply. Sample section: Twin steel manifolds with ballast, B, service either of two inlets to the reactor. The sample is placed in a 64 cc glass pyrolysis tube equipped with Kovar adapted Varian flanges. Temperature control is provided by a clam-shell furnace and thermocouple, TC. Vernier valves at the inlet and outlet are calibrated for an operating pressure of 100 Torr, measured by a 100 Torr Barocel head, P. The glass reactor is configured with twin quartz windows, V, and twin, switchable, sample inlets, and is vented (black arrow) through a 2 in line by a roots blower capable of 126 cfm pumping speed. A 10 cm monochromator (J-Y Mod. H-10, ISA Inc., Metuchen, NJ), disperses 200-800 nm light into an EMI 9789QB photomultiplier, PM, equipped with shutter, S, and configured for photon-counting (PAR Quantometer Mod. 1140A).

impurities. The latter is both an indicator of the relative argon metastable concentration, and a proof of presence of the $Ar(^3P_2)$ state when no higher than the second vibrational level of the $N_2(C^3\Pi_u)$ state is represented (ref.9), which at 11.5 eV matches the energy of the metastable argon state. A vestige of argon lines (e.g., 404-430 nm) was attributed to a reflection of the plasma port from the rear viewing window. The spectral behavior is qualitatively understandable by noting that the cathode glow extends over the cathode surface towards the optical viewing region, and the current and pressure determine this extent (ref. 5). Low pressures and high currents permit short-lived decay processes to interfere spectrally. The pressure regime selected for this study is consistent with that of others (refs. 4, 6). The reactor interior had been gold plated for another purpose and although removal of the gold by sputtering was confirmed by the detection of emission lines for Au(I) and Au_2, spectra of material from Kovar or steel were not observed.

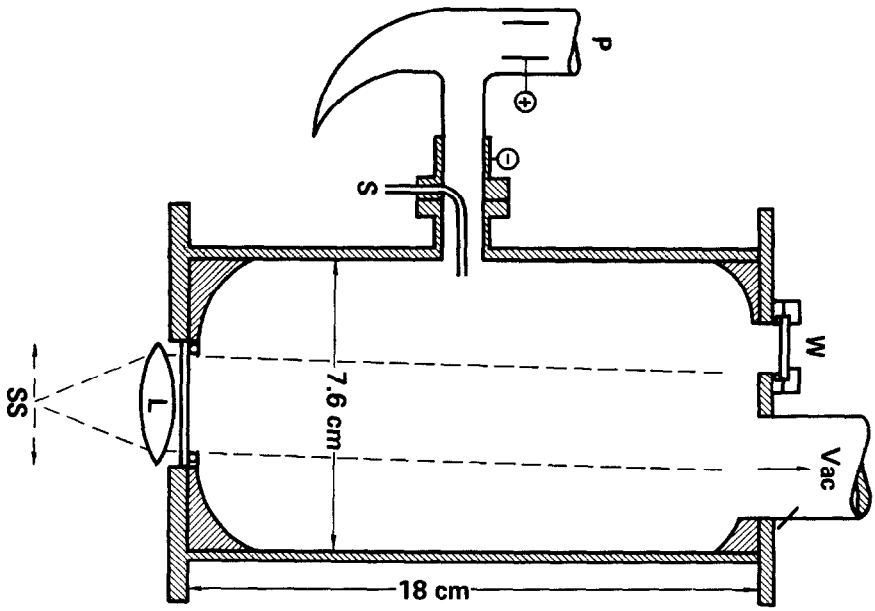

Fig.2. Steel reactor configuration. The plasma gas is discharged between a tantalum shell in plasma tube, P, and the reactor at the attachment flange, which acts as a cathode. Sample enters at S, through a brazed plasma flange tube fitting. The glow discharge remains in the flange area. The rear viewport, W, serves for visual and calibration purposes. The spectrometer slit (SS) placement relative to 100 mm quartz collimating lens, L, allows a traversing view of the reactor interior.

Table 2. Experimental parameters and operating conditions in this study.

Glow voltage	200 V
Glow current	1-25 mA
Reactor pressure	0.5, 1.0 Torr
Plasma flow	522 μmol/s
Carrier flow	1-30 μmol/s
Pyrolysis tube	64 cc
Tube carrier pressure	100 Torr
Linear flow	180, 220 m/s

Moisture

Both argon amd helium plasmas are suitable for determination of water, using the 308.9-nm or 283-nm OH bands. Table 3 contains an example of replications of calibration injections that were achieved with a standard

Table 3. Behavior of injected water samples using a helium-flowing afterglow. Sets A, B, C differ from each other in operating conditions. A illustrates replication. B shows loss with increased carrier flow. C shows recovery with manual control (c) of the flow.

Set	Taken µg	Carrier flow µmol/s	Integral V-s
A	5	31	12.6
	5	31	10.8
	5	31	11.0
	5	31	11.4
B	20	10	93.
	20	3.5	137.
	20	1.1	143.
C	20	(c)	32.
	30	(c)	63.
	60	(c)	123.

deviation of 7 percent in a set of four. Poorly-performed injections resulted in the simultaneous introduction of excessive amounts of air. This was evidenced by a rapid increase in the nitrogen band intensity. The carrier gas flow rate was then varied for the same size sample. The integral is replicated except when high flows or large samples were employed. The data suggest that saturation of available metastables limit the maximum rate of introduction of water. To test this, a large 60 µg sample of water was introduced, but the carrier flow was controlled manually to prevent saturation. Acceptable values were again obtained, but at the expense of a long, 20 min. integration time. This practical upper limit constrains the use of batch analysis to relatively small amounts of solids. For example, the difficulty of anticipating rapid water evolution was experienced in attempts to determine water in sodium tartrate dihydrate (15.66 percent water, 90-160°C). A 7 mg sample (1 mg water) was heated at 2°C/min., with a recovery of less than 25 percent. The saturation level estimated from the time traces corresponds to a metastable population of ca. 10 nmol/s, which is 2×10^{-5} of the plasma flow. This is somewhat below the figure of 10^{-4} quoted by Setzer (ref. 4).

From the calibration data, the sensitivity for water in a 1 Torr argon plasma, using 14 mA source current, 0.05 mm slits (0.4 nm bandpass) and the 308.9 nm OH band was determined to be 30000 photon counts/nmol with a 0.5 µg sample. In helium, 5200 counts/nmol were obtained for the same conditions.

The ratio agrees reasonable with the ratio of corresponding ion-water molecule reaction rate constants (ref. 7).

This high sensitivity makes possible the steady state, or isothermal detection of very small amounts of moisture, such as that produced by decomposition. Determinations are not so much limited by the sensitivity for OH as the behavior of residual water in the system. The lowest blanks were estimated to be 0.2 nmol/s (0.4 ppm). Frequently, system leaks in the order of 0.5 nmol/s (10^{-5} scc/s) could be inferred from the presence of nitrogen bands. With only a 100 Torr Barocel and thermocouple gauge to measure pressure, such leaks were hard to detect, therefore, these bands became the most sensitive criteria for air leaks. Although the nitrogen bands virtually disappeared when care was taken to insure a leak-free system, the OH residual from virtual leaks remained.

To explore the analytical limits, an attempt was made to detect moisture evolving from a nitrocellulose, which had been outgassed in vacuo for 24 hr at 60°C. The OH residual was measured in a helium plasma with and without sample in the pyrolysis tube, and with a reference stream of carrier gas. With 0.5-gm sample present, an increase in the OH band intensity was the only distinquishable spectral difference, corresponding to 0.9 nmol/gm-s or twice the blank. This is similar to the rate measured for NO_x (ref. 8). In contrast with larger amounts of moisture, the OH intensity did not vary linearly with the carrier flow rate, and reached a constant value for carrier flows in excess of 3 mol/s. With injected or batch samples, Eq. 1 expresses the exponential decay of the signal, S, which is proportional to the carrier flow, C. In steady-state measurements, Eq. 2 expresses the independence of signal on carrier flow, unless the fraction of impurity, f, in the carrier is large. Both equations can easily be derived from mass balance considerations in a fixed volume, flow-through tube.

$$\text{Eq. (1)} \quad S = k(C/PV)n_0 \exp(-t/\tau)$$

$$\text{Eq. (2)} \quad S = k\,(\dot{n}_s + fC)$$

where k is a proportionality constant
C is the carrier flow, mol s^{-1}
PV is the carrier present in the tube, mol
n_0 is the initial amount analyte, mol
τ is the time constant for the tube, = PV/C
$\dot{n}_s$ is the rate of evolution of analyte from a solid sample
f is the fractional constant of analyte in the carrier.

The Glass Reactor

The glass reactor was constructed as a module, so that it could easily adapt to the existing system. This had one important electrical consequence: because of a steel vacuum manifold downstream of the source, a conductive path through the reactor occurred, and is discussed below. Other differences from the steel reactor were 1) smaller dimensions, resulting in an estimated eight-fold reduction in the residence time, 2) closer proximity of walls in the plasma inlet (0.4 cm^2 vs 2 cm^2), 3) an annular sample inlet rather than axial (diffusion alone caused mixing), 4) twin view windows permit more flexibility, and 5) a secondary sample inlet was available, but not employed in this work.

Preliminary studies showed very limited sensitivity for OH and N_2 with either helium or argon. This is shown in Fig. 3, where the largest signals occur with a 1 mA discharge current, as described by Stedman and Setzer (ref. 4). The maximum, however was some 20-fold less than the best obtained with the steel reactor (at 14 mA).

Subsequently, an accidental excess of nitrogen was added while the discharge was operating at a high current (50 mA). Black deposits formed on the reactor inlet and were presumed to be sputtered tantalum. Thereafter, the luminous afterglow extended as far as the sample inlet port, and the sensitivity improved markedly. Furthermore, a linear improvement in signal at the downstream window was obtained on increasing the current to 25 mA, as shown in Fig. 3. Under these conditions, weak helium or argon spectra were also observed.

Although the downstream vacuum manifold was electrically isolated by a 3 cm section of glass tube, the appearance of a glow in this section, more than 1 metre from the source is direct evidence of a current path through the reactor. It may be surmised that the increased ion flux, which also can fragment impurities, contributed to increased sensitivity. Additionally, the dark coating may have conditioned the glass walls to cause less destruction of metastables. These effects remain to be investigated.

CONCLUSIONS

The use of the steel reactor configuration of Fig. 2 has not been reported, probably because reaction kinetic studies, for which FLAG is most often employed, must avoid ion-molecule reactions and photolysis as secondary processes. However, for analytical purposes, these processes did not appear to adversely affect selectivity, and probably contribute to sensitivity. The steel reactor and plasma tube are easier to construct, and improved

sensitivity over that of a glass reactor was obtained. This was largely attributable to an increased residence time of the chemiluminescent plume in the viewing aperature. Higher currents can be employed to increase the available metastable population. Elimination of leaks also would help. In this study, range was recovered by controlling the carrier flow during the determination.

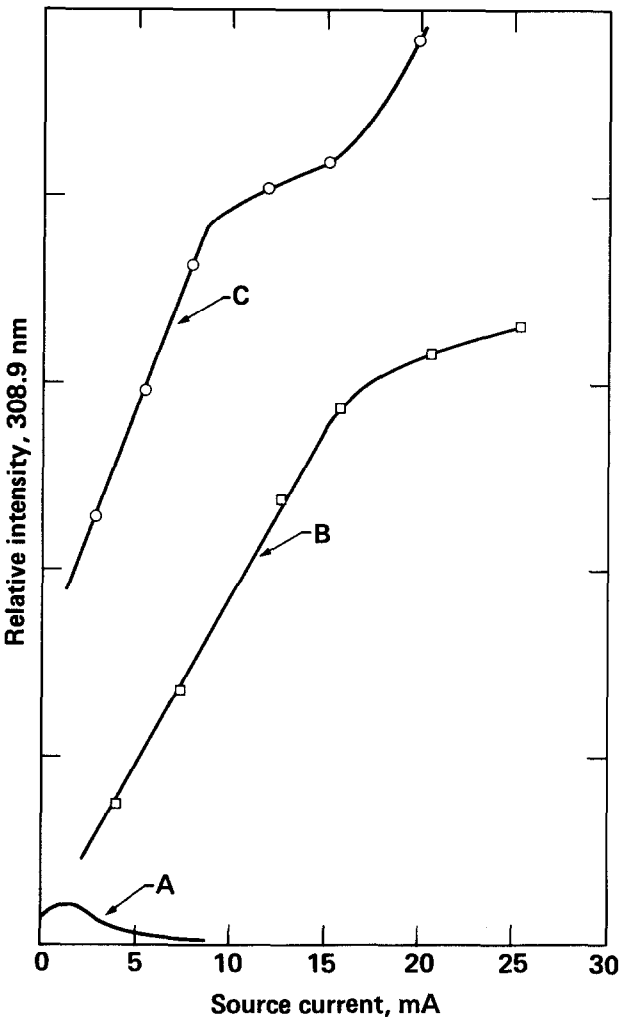

Fig. 3. Argon discharge current dependence of the intensity of 308.8 nm (OH). A. Glass reactor, 0.05 mm slit, before conditioning. B. glass reactor, 0.5 mm slit, after conditioning. C. Steel reactor, 0.05 mm slit.

Steel has disadvantages as a material for a water detector. Although it is bakable, it absorbs moisture easily, and subsequently releases water in flowing gases, resulting in a virtual leak. This limits the full potential of the FLAG technique in its application to trace moisture. However, FLAG appears superior to other methods, such as quantitative mass spectroscopy, which is even more subject to adsorption losses of moisture.

REFERENCES

1. R. J. Copeland, MHSMP-81-02, Pantex, Amarillo, TX, Jan. 1981.
2. G. H. Andrews, R. N. Rogers, and G. W. Taylor, "TATB Thermal Decomposition Kinetics," 5th ERDA Compatibility Conference, Mound Lab., Miamisburg, OH, Oct. 4-6, 1977.
3. G. W. Taylor, J. Phys. Chem. 77, 124 (1973).
4. D. H. Stedman and D. W. Setzer in PROGRESS IN REACTION KINETICS, K. R. Jennings, ed., (Pergamon Press, New York, New York, 1971), Part 4, Vol. 6, pp. 193-239.
5. F. Llewellyn-Jones, THE GLOW DISCHARGE, (J. Wiley, New York, 1966).
6. J. M. Cook, T. A. Miller, and V. E. Bondybey, J. Chem. Phys. 68, 4 (1978).
7. E. E. Ferguson, Atomic Data and Nuclear Data Tables 12, 159 (1973).
8. H. N. Volltrauer and A. Fontijn, Combustion and Flame 41, 313 (1981).
9. D. H. Stedman and D. W. Setzer, J. Chem. Phys. 52, 3957 (1970).